THE JOURNAL OF BIOLOGICAL CHEMISTRY VOL. 283, NO. 52, pp. 36088–36099, December 26, 2008

In Skeletal Muscle Advanced Glycation End Products (AGEs) Inhibit Insulin Action and Induce the Formation of Multimolecular Complexes Including the Receptor for AGEs*

Received for publication, March 3, 2008, and in revised form, October 16, 2008 Published, JBC Papers in Press, October 27, 2008, DOI 10.1074/jbc.M801698200

Angela Cassese[‡1], Iolanda Esposito[‡1], Francesca Fiory[‡], Alessia P. M. Barbagallo[‡], Flora Paturzo[‡], Paola Mirra[‡], Luca Ulianich[‡], Ferdinando Giacco[‡], Claudia Iadicicco[‡], Angela Lombardi[‡], Francesco Oriente[‡], Emmanuel Van Obberghen[§], Francesco Beguinot[‡], Pietro Formisano[‡], and Claudia Miele[‡2]

From the [‡]Dipartimento di Biologia e Patologia Cellulare e Molecolare and Istituto di Endocrinologia ed Oncologia Sperimentale del Consiglio Nazionale delle Ricerche, Università degli Studi di Napoli Federico II, Naples 80131, Italy and [§]INSERM U907 (ex U145), IFR 50, Faculté de Médecine, Université de Nice Sophia-Antipolis, Nice, 06107 France

Chronic hyperglycemia promotes insulin resistance at least in part by increasing the formation of advanced glycation end products (AGEs). We have previously shown that in L6 myotubes human glycated albumin (HGA) induces insulin resistance by activating protein kinase Cα (PKCα). Here we show that HGA-induced PKCα activation is mediated by Src. Coprecipitation experiments showed that Src interacts with both the receptor for AGE (RAGE) and PKCα in HGA-treated L6 cells. A direct interaction of PKCα with Src and insulin receptor substrate-1 (IRS-1) has also been detected. In addition, silencing of IRS-1 expression abolished HGA-induced RAGE-PKCα co-precipitation. AGEs were able to induce insulin resistance also *in vivo*, as insulin tolerance tests revealed a significant impairment of insulin sensitivity in C57/BL6 mice fed a high AGEs diet (HAD). In tibialis muscle of HAD-fed mice, insulin-induced glucose uptake and protein kinase B phosphorylation were reduced. This was paralleled by a 2.5-fold increase in PKCα activity. Similarly to *in vitro* observations, Src phosphorylation was increased in tibialis muscle of HAD-fed mice, and co-precipitation experiments showed that Src interacts with both RAGE and PKCα. These results indicate that AGEs impairment of insulin action in the muscle might be mediated by the formation of a multimolecular complex including RAGE/IRS-1/Src and PKCα.

Insulin resistance is genetically determined, but it may also be affected by environmental conditions and by factors secondary to diseases (1). These acquired and secondary factors further impair insulin action in diabetic individuals. For instance, chronic hyperglycemia *per se* promotes insulin resistance (2, 3). A number of mechanisms have been proposed to explain hyperglycemia-induced insulin resistance. These include abnormalities in the protein kinase C (PKC)[3] signaling system (4) and activation of the NF-κB transcription factors by chronically elevated glucose concentrations (5, 6). Chronic hyperglycemia also leads to the production of Amadori products through the nonenzymatic glycation reactions between glucose and reactive amino groups of serum proteins. Depending on the protein turnover rate and glucose concentration, Amadori products undergo further irreversible reactions to form advanced glycation end products (AGEs). The modifications of proteins that lead to their glycation induce alterations in biological properties as compared with their non-glycated counterparts. Several studies have shown that elevated concentrations of Amadori products such as glycated albumin (GA) are associated with diabetic atherogenesis by activating vascular smooth muscle cells (7). GA has also been implicated in the development of diabetic retinopathy (8) by induction of vascular endothelial growth factor expression (9, 10) and the stimulation of choroidal endothelial cell proliferation (11). Finally, GA has been shown to participate in the development of diabetic nephropathy by the induction of cytokines and growth factors (12), which may themselves contribute to diabetic renal disease (13). In addition to those endogenously formed, AGEs are abundant in exogenous sources such as foods, especially when prepared under elevated temperatures (14, 15). After ingestion, 10% of preformed AGEs are absorbed into the human or rodent circulation (16, 17), ⅔ of which are retained in tissues. Also, reduced intake of dietary AGEs has been shown to

* This work was supported by the European Foundation for the Study of Diabetes and the GlaxoSmithKline Programme for the Study of Metabolic Toxicity in Diabetes, Consiglio Nazionale delle Ricerche Grant RSLT, European Community FP6 EUGENE2 Grant LSHM-CT-2004-512013 and PREPOBEDIA, by grants from the Associazione Italiana per la Ricerca sul Cancro, and by the Ministero dell'Università e della Ricerca Scientifica Grants PRIN and FIRB RBNE0155LB. The work in Nice was supported by European Community FP6 EUGENE2 Grant LSHM-CT-2004-512013, the INSERM, Université de Nice-Sophia-Antipolis, Conseil Régional PACA and Conseil Général des Alpes-Maritimes, the Fondation de France (Paris, France, 2007–2008), and the PRND (Programme de Recherche Nationale sur le Diabète, France, 2003-2007). The costs of publication of this article were defrayed in part by the payment of page charges. This article must therefore be hereby marked "*advertisement*" in accordance with 18 U.S.C. Section 1734 solely to indicate this fact.

[1] Both authors contributed equally to this manuscript.

[2] To whom correspondence should be addressed: Istituto di Endocrinologia ed Oncologia Sperimentale-CNR and DBPCM Università di Napoli Federico II, Via Sergio Pansini 5, Naples 80131, Italy. Tel.: 39-081-746-3248; Fax: 39-081-746-3235; E-mail: c.miele@ieos.cnr.it.

[3] The abbreviations used are: PKC, protein kinase C; PKB, protein kinase B; AGE, advanced glycation end product; RAGE, receptor for AGE; sRAGE, soluble RAGE; GA, glycated albumin; HGA, human GA; PP1, 4-amino-5-(4-methylphenyl)-7-(*t*-butyl)pyrazolo[3,4-d]-pyrimidine; CML, carboxymethyllysine; LAD, low AGE diet; HAD, high AGE diet; PLD, phospholipase D; HA, human serum albumin; MAPK, mitogen-activated protein kinase; ERK, extracellular signal-regulated kinase; IRS-1, insulin receptor substrate-1; PBS, phosphate-buffered saline; DAG, diacylglycerol; DN, dominant negative.

decrease the incidence of type 1 diabetes in non-obese diabetic mice (18) as well as the formation of atherosclerotic lesions in diabetic apolipoprotein E-deficient mice (19). Furthermore, Vlassara and co-workers (20) have shown that reduced AGE intake leads to lower levels of circulating AGEs and to improved insulin sensitivity in *db*/*db* mice. Several AGE-binding proteins have been identified, including lactoferrin, galectin-3 (AGE-R3), lysozyme, and the receptor for AGE (RAGE) (21). RAGE is a multiligand member of the immunoglobulin superfamily and is expressed on the surface of a variety of cell types. By their binding to RAGE, AGEs trigger a range of cellular responses. RAGE has been reported to activate intracellular signals including the MAPK cascade and the cdc42/Rac pathway (22), leading to amplification or progression of various diseases including diabetic vascular complications (23), inflammation (24), and tumor growth/metastasis (25). The cytoplasmic region of RAGE is considered to be responsible for the binding of the signaling molecule(s) (26). It has been demonstrated that ERK1/2 interacts with the cytoplasmic region of RAGE after stimulation with amphoterin (27). Furthermore, recent studies have shown that STAT5 becomes activated and physically interacts with RAGE upon glycated low density lipoprotein stimulation (28). However, RAGE is devoid of intrinsic catalytic activity. Src tyrosine kinase is required for signaling events downstream of several receptors lacking intrinsic tyrosine kinase activity, such as cytokine receptors. Cho *et al.* (29) have shown that glycated low density lipoprotein (LDL) activates ERK1/2 via Src-, phospholipase C (PLC)-, and PKC-dependent pathways, whereas native and non-glycated LDL activate ERK1/2 by an Src-independent mechanism. It has been recently reported that in vascular smooth muscle cells derived from insulin-resistant and diabetic *db/db* mice, RAGE expression and Src activity are increased compared with those from control mice. Further studies showed that the RAGE ligand S100B induced Src activation in a RAGE-dependent manner. Moreover, in vascular smooth muscle cells Src activation is necessary for the S100B-induced RAGE downstream signaling involving several targets such as caveolin-1, MAPKs, NF-κB, and STAT3. Interestingly, a PKC inhibitor could block S100B-induced activation of MAPKs, suggesting a role for PKC in this event (30). Recently, we have demonstrated that human glycated albumin (HGA) pretreatment induces a selective activation of PKCα. Insulin receptor substrate (IRS) serine/threonine phosphorylation by HGA-activated PKCα inhibits insulin-stimulated glucose metabolism without changes in growth-related pathways regulated by insulin (31). However, the intracellular signaling mechanism by which HGA induces PKCα activation remains to be determined. In this work we report that HGA and dietary AGEs induce the formation of a complex including RAGE, PKCα, and Src in L6 cells and in skeletal muscle from insulin-resistant HAD-fed mice, respectively. In L6 cells HGA-mediated complex formation requires the presence of IRS-1. We suggest that the formation of this complex may mediate the AGE-dependent inhibition of insulin action in skeletal muscle cells *in vitro* and, possibly, *in vivo*.

EXPERIMENTAL PROCEDURES

General—Media, sera, antibiotics for cell culture, and the Lipofectamine reagent were from Invitrogen (Invitrogen). Phospho-PKB and phospho-Src antibodies were purchased from Cell Signaling Technology, Inc. (Beverly, MA). PKB, IRS-1, phospho-Ser^{657} PKCα, phospho-Tyr antibodies were purchased from Upstate Biotechnology, Inc. (Lake Placid, NY). PKCα, PKCβ, PKCδ, PKCζ, and RAGE antibodies were from Santa Cruz Biotechnology Inc. (Santa Cruz, CA). Src antibody was from Calbiochem (EMD Chemicals, Inc. San Diego, CA). The PKC assay system was from Promega (Madison, WI). Protein electrophoresis reagents were purchased from Bio-Rad, and ECL reagents were from GE Healthcare. The IRS-1 ribozyme and control ribozyme were generous gifts of M. Quon (National Institutes of Health, Bethesda, MD). PP1 (4-amino-5-(4-methylphenyl)-7-(t-butyl)pyrazolo[3,4-d]-pyrimidine) was from Alexis Biochemicals (San Diego CA). Soluble RAGE was kindly provided by A. Bierhaus (University of Heidelberg, Heidelberg, Germany). All other chemicals were from Sigma.

Cell Culture and Transfection—The L6 skeletal muscle cells were plated (6×10^3 cells/cm^2) and grown in Dulbecco's modified Eagle's medium containing 1 g/liter glucose supplemented with 2% (v/v) fetal bovine serum and 2 mM glutamine. Cultures were maintained at 37 °C in a humidified atmosphere containing 5% (v/v) CO_2. Under these culture conditions, L6 myoblasts spontaneously differentiate into myotubes upon confluence. Transient transfections of IRS-1 and control ribozymes and of the kinase-inactive Src were performed by the Lipofectamine method according to the manufacturer's instruction. The cells were incubated for the appropriated times with 0.1 mg/ml of HGA or non-glycated human serum albumin (HA) as a control. Where indicated, cells were pretreated for 1 h with 50 μM PD98059, 30 min with 50 nM wortmannin, 2 h with 5 μM PP1, or 30 min with 10 μM U73122 or 5 μM U73343 before the incubation with HGA. Where indicated, 50 μg/ml of soluble RAGE (sRAGE) were added together with HGA for the appropriated times (32).

Characterization of Glycated Human Serum Albumin—Glycated and nonglycated human serum albumin were purchased from Sigma. The glycated serum albumin contained 2–5 mol of fructosamine/mol of albumin. The human glycated and nonglycated albumin preparations were tested for carboxymethyllysine (CML) concentrations and the extent of lysine and arginine modifications as already described (31). Each batch was tested for possible insulin-like growth factor-I contamination by IGF-I-D-RIA-CT (BioSource Europe, Nivelles, Belgium) and the absence of endotoxin (lipopolysaccharide) by the use of Limulus amebocyte lysates assay (Sigma). Each human glycated albumin batch was reconstituted at 10 mg/ml with sterile PBS and, to avoid glycoxidation, thereafter immediately frozen at −30 °C until use. The results obtained are summarized in Table 1 and show the absence of significant modifications in the extent of free lysine and arginine residues between the two preparations. Furthermore, the batches were found not to contain IGF-I and to be bacterial endotoxin-free. The physicochemical properties determined for our HGA preparation demonstrate that the effects observed in L6 myotubes are the

TABLE 1
Characteristics of glycated human albumin
Modification ratio of HGA was expressed as a percent of non-glycated human albumin modifications used as control.

	Non-glycated human albumin	Glycated human albumin
CML/mg protein	55 ng	195 ng
Lys modification (%)	100	94.9 ± 3.2
Arg modification (%)	100	91.6 ± 1.5
IGF-1	Undetectable	Undetectable
LPS	Undetectable	Undetectable

TABLE 2
Characteristics of HAD and LAD

Nutrients	HAD	LAD
Protein (%)	20.5	18.5
Fat (%)	4.7	4.0
Carbohydrate (%)	54.8	58.6
Fiber (%)	5.5	6.0
Niacin (mg/kg)	93	55
Folic acid (mg/kg)	2.9	1.92
Pantothenic acid (mg/kg)	17	14,4
Biotin (mg/kg)	0.1	0.279
Cholin (mg/kg)	1000	1000
Vitamin A (IU/kg)	2500	4400
Vitamin D3 (IU/kg)	2200	1260
Vitamin E (IU/kg)	99	49.5
Vitamin B1 (mg/kg)	18	13.5
Vitamin B2 (mg/kg)	8	6.74
Vitamin B6 (mg/kg)	7.8	5.98
Vitamin B12 (mg/kg)	0.018	0.027
Caloric profile (kcal/g)	3.4	3.7

consequence of glycated albumin present essentially as a glycated Amadori product.

Immunoblotting, Overlay Blot, PKC Assay, and Determination of Diacylglycerol (DAG) Cellular Content—Cell lysates were solubilized as described in Miele *et al.* (31). Mice were sacrificed by cervical dislocation, and tibialis and soleus muscle samples were collected rapidly and homogenized as previously reported (33). Tissue homogenates and cell lysates were then separated by SDS-PAGE and analyzed by Western blot as described (34). Cell lysates immunoprecipitations were accomplished as described in Oriente *et al.* (35). Overlay blotting with biotinylated PKCα was performed as reported previously (34). Filters were revealed by ECL and autoradiography. Upon immunoprecipitation with anti-PKCα or anti-RAGE antibodies, PKC activity was assayed using the SignaTECT PKC assay system (Promega) according to the manufacturer's instructions as described in Oriente *et al.* (35). DAG content was quantified radioenzymatically by incubating aliquots of the lipid extract with DAG kinase and [^{32}P]ATP as described previously (36, 37).

Animals and Treatment— 4-Week-old C57/BL6 female mice (*n* 20) were purchased from the Charles River Laboratories (Milan, Italy). Animals were kept under a 12-h light/12-h dark cycle, and all experimental procedures and euthanasia described below were approved by Institutional Animal Care and Utilization Committee. After 1 week of adjustment, C57/BL6 mice were randomly divided into two groups and placed for 20 weeks on two commercially available standard rodent diets similar in nutritional and caloric content (Table 2) but with different AGEs content. Research Diets formula D12328 (Research Diets, Inc., New Brunswick, NJ) was used for the low AGE diet (LAD), and PicoLab Rodent Diet 20 exposed to an additional step of autoclaving at 120 °C for 30 min (Labdiet; Purina Mills, St. Louis, MO) was used for the high AGE diet (HAD) (20). Fasting blood glucose and body weights were monitored biweekly. After 1 week of adjustment, food intake (in grams of food) of individual mice was recorded daily for 1 week at week 1, 11, and 22.

Skeletal muscles (quadriceps) of a group of 12 age-matched C57/BL6 mice were injected with 50 mg/kg glycated albumin (4 mice), non-glycated albumin (4 mice), or PBS (4 mice). Another group of 12 mice were treated with the same concentrations of glycated and non-glycated albumin, but the compounds were delivered by tail vein injection. Mice were sacrificed after 24 h by cervical dislocation, and muscle samples were collected rapidly and homogenized as previously reported (33).

AGEs Determination, Metabolite Assays, and 2-Deoxy-D-[1-^{3}H]Glucose Uptake in Vivo—CML concentrations were determined by using a CML-enzyme-linked immunosorbent assay kit as described in Miele *et al.* (31). Fasting and fed blood glucose levels were measured with glucometer (A. Menarini Diagnostics, Florence, Italy). Insulin tolerance tests, glucose tolerance tests, and serum insulin measurements were performed as previously described (33). Fasting plasma free fatty acid levels were measured with Wako NEFA C kit (Wako Chemicals, Richmond, VA), and triglycerides were measured with the Infinity triglyceride reagent (Sigma-Aldrich). For analyzing glucose utilization by skeletal muscle, an intravenous injection of 1μCi of the non-metabolizable glucose analog 2-deoxy-D-[1-^{3}H]glucose (GE Healthcare) and an intraperitoneal injection of insulin (0.75 milliunits/kg of body weight) were administered to random-fed mice. The specific blood 2-deoxy-D-[1-^{3}H]glucose clearance was determined with 25-μl blood samples collected from the tail vein obtained 1, 15, and 30 min after injection as previously reported (33).

Statistical Analysis—Data were analyzed with Statview software (Abacus Concepts) by one-factor analysis of variance and are expressed as the means ± S.D. Statistical significance was evaluated using Student's *t* test for unpaired comparison. A value of $p < 0.05$ was considered statistically significant. The total area under the curve for glucose response during the insulin tolerance tests and the glucose tolerance tests was calculated by the trapezoidal method.

RESULTS

Role of HGA-activated Src in PKCα Activation in L6 Skeletal Muscle Cells—To investigate the molecular mechanisms of PKCα activation by AGEs, HGA-induced PKCα activity was measured in L6 cells treated with different pharmacological inhibitors to selectively block ERK1/2, phosphatidylinositol 3-kinase, and Src. PKCα activity in response to HGA was unchanged upon treatment of L6 cells with PD98059 and wortmannin, which inhibit ERK1/2 and phosphatidylinositol 3-kinase, respectively (Fig. 1*a*). At variance, preincubation with the Src inhibitor PP1 or the expression of a dominant negative kinase-inactive Src (SrcDN) (38) reduced by almost 70% HGA-induced PKCα activity (Fig. 1*a*). Therefore, the levels of Src phosphorylation on Tyr^{416} have been evaluated in L6 myotubes upon incubation for 24 h with HGA in the presence or absence of either PP1 or SrcDN. Src phosphorylation was increased by

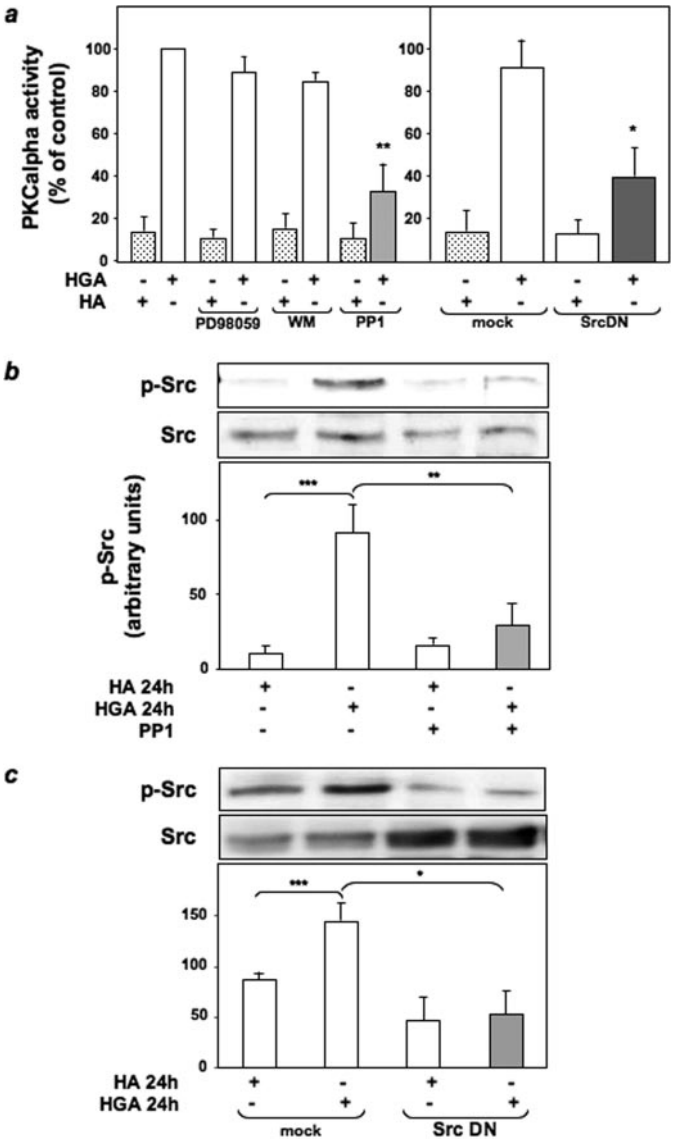

FIGURE 1. **HGA-activated Src mediates PKCα activation in L6 skeletal muscle cells.** *a*, L6 skeletal muscle cells were incubated with 0.1 mg/ml HA or HGA for 24 h in the absence or in the presence of 50 μM PD98059, 50 nM wortmannin (*WM*), or 5 μM PP1. PKCα activity was assayed in the immunoprecipitates as described under "Experimental Procedures." PKCα activity was measured also in L6 cells transfected with the empty vector pSG5 (*mock*) or with the vector pSG5 expressing a kinase-inactive Src protein (*SrcDN*) and then incubated with 0.1 mg/ml HA or HGA for 24 h. *Bars* represent the mean $\pm$ S.D. of three independent experiments. *b*, L6 cells were incubated with 0.1 mg/ml HA or HGA for 24 h in the absence or in the presence of 5 μM PP1, lysed as described under "Experimental Procedures"; lysates were then separated by SDS-PAGE followed by immunoblotting with antibodies to phosphotyrosine 416 Src or total Src. The autoradiographs shown are representative of four independent experiments. *c*, cell lysates of L6 skeletal muscle cells transfected with the empty vector pSG5 (*mock*) or with the vector pSG5 expressing a kinase-inactive Src protein (*SrcDN*) and treated as in *b* were then separated by SDS-PAGE followed by immunoblotting with antibodies to phosphotyrosine 416 Src or total Src. The autoradiographs shown are representative of three independent experiments. *, statistically significant differences (*, $p < 0.1$; **, $p < 0.01$; ***, $p < 0.001$).

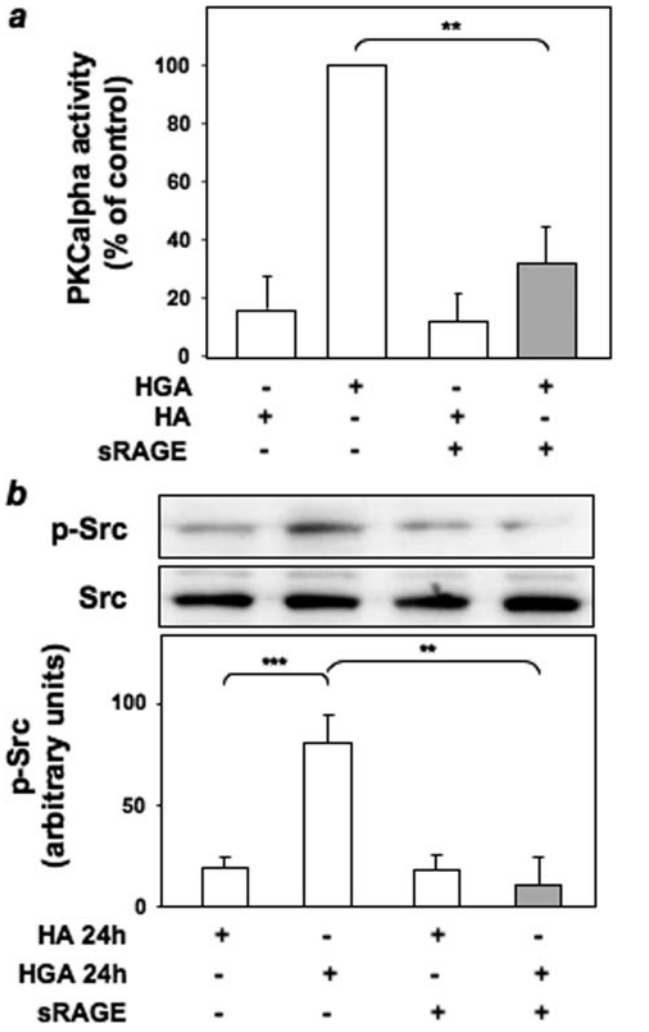

FIGURE 2. **sRAGE abrogates HGA-activated Src and PKCα activation in L6 skeletal muscle cells.** *a*, L6 skeletal muscle cells were incubated with 0.1 mg/ml HA or HGA for 24 h in the absence or in the presence of 50 μg/ml sRAGE. PKCα activity was assayed in the immunoprecipitates as described under "Experimental Procedures." *Bars* represent the mean $\pm$ S.D. of three independent experiments. *b*, L6 skeletal muscle cells were incubated with 0.1 mg/ml HA or HGA for 24 h in the presence or in the absence of 50 μg/ml sRAGE, lysed as described under "Experimental Procedures"; lysates were then separated by SDS-PAGE followed by immunoblotting with antibodies to phosphotyrosine 416 Src or total Src. The autoradiographs shown are representative of three independent experiments. *, statistically significant differences (**, $p < 0.01$; ***, $p < 0.001$).

HGA, but this effect was prevented by PP1 treatment (Fig. 1*b*) and by overexpression of SrcDN (Fig. 1*c*). Furthermore, both HGA-induced PKCα (Fig. 2*a*) and Src (Fig. 2*b*) activation were inhibited by the addition of an excess of sRAGE. To investigate the possibility that HGA-activated Src could directly regulate PKCα activity, we first measured in L6 myotubes PKCα tyrosine phosphorylation after HGA incubation for 24 h. As shown in Fig. 3*a*, HGA induced a 3-fold increase of the tyrosine phosphorylation of PKCα. This effect was abolished in the presence of PP1.

Role of PLC and Phospholipase D (PLD) in HGA-induced PKCα Activation in L6 Skeletal Muscle Cells—DAG is the main endogenous activator of classical PKCs (37). We, therefore, performed thin-layer chromatography to evaluate DAG levels in response to HGA treatment for 24 h in the presence or absence of PP1. HGA caused a >5-fold increase ($p < 0.001$) in the amount of DAG in L6 skeletal muscle cells. Interestingly, the HGA effect on DAG levels was significantly reduced ($p < 0.001$) when cells were treated with PP1 (Fig. 3*b*). In response to extracellular stimuli, DAG is mainly generated through the action of PLC and PLD (37). To clarify the role of PLC and PLD in HGA-

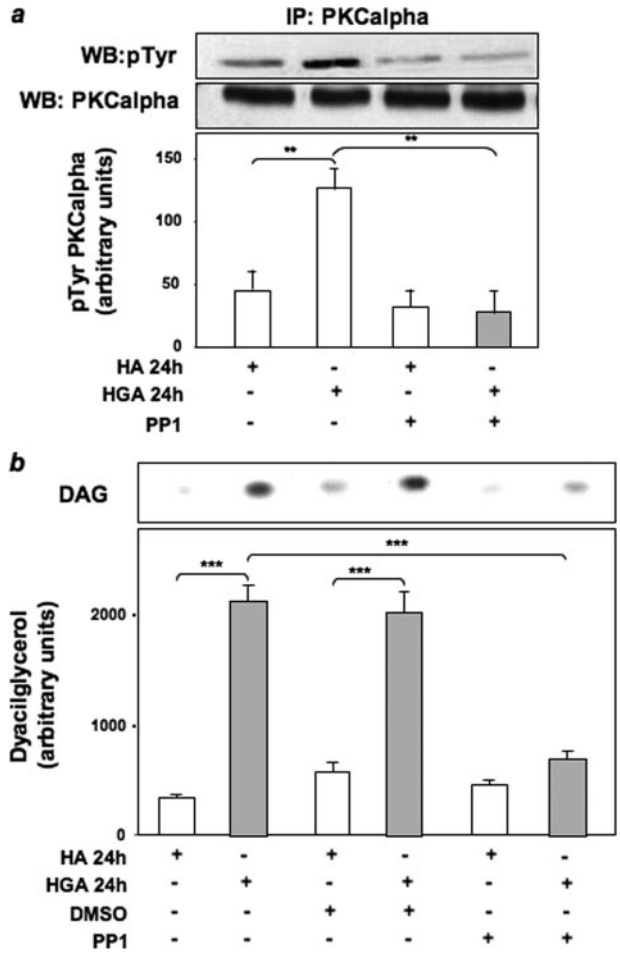

FIGURE 3. **Role of Src in HGA-induced PKCα activation in L6 skeletal muscle cells.** *a*, lysates from L6 skeletal muscle cells treated or not with 0.1 mg/ml HA or HGA for 24 h in the absence or in the presence of 5 μM PP1 were precipitated (*IP*) with selective anti-PKCα antibodies and immunoblotted (*WB*) with anti-phosphotyrosine or anti-PKCα antibodies. The autoradiographs shown are representative of three independent experiments. *b*, L6 skeletal muscle cells were incubated with 0.1 mg/ml HA or HGA for 24 h in the absence or in the presence of 5 μM PP1. Lipids were extracted, and determination of DAG levels was performed as described under "Experimental Procedures." [^{32}P]Phosphatidic acid was separated by TLC and quantitated by densitometric analysis. *Bars* represent the mean ± S.D. of values obtained from three independent experiments in duplicate. The autoradiographs shown are representative of three independent experiments. *, statistically significant differences (**, $p < 0.01$; ***, $p < 0.001$).

induced PKCα activation, we evaluated PKCα phosphorylation levels in L6 cells treated or not with the PLD1 inhibitor 1-butanol, the PLC inhibitor U73122, and its inactive structural analogue U73343. PKCα activation, measured as Ser^{657} phosphorylation, was unaffected by preincubation with 1-butanol but was abolished by treatment with U73122 (Fig. 4*a*). By contrast, treatment with U73343 did not modify HGA effect on PKCα phosphorylation (Fig. 4*b*).

HGA-induced Association of PKCα, Src, and RAGE in L6 Skeletal Muscle Cells—To investigate the ability of HGA to induce the formation of a molecular complex between Src, RAGE, and/or PKCα, lysates from HGA-stimulated or untreated L6 myotubes were precipitated with anti-RAGE antibody and blotted with anti-Src or anti-PKCα antibodies. As shown in Fig. 5*a*, HGA treatment increased RAGE coprecipitation with both Src and PKCα.

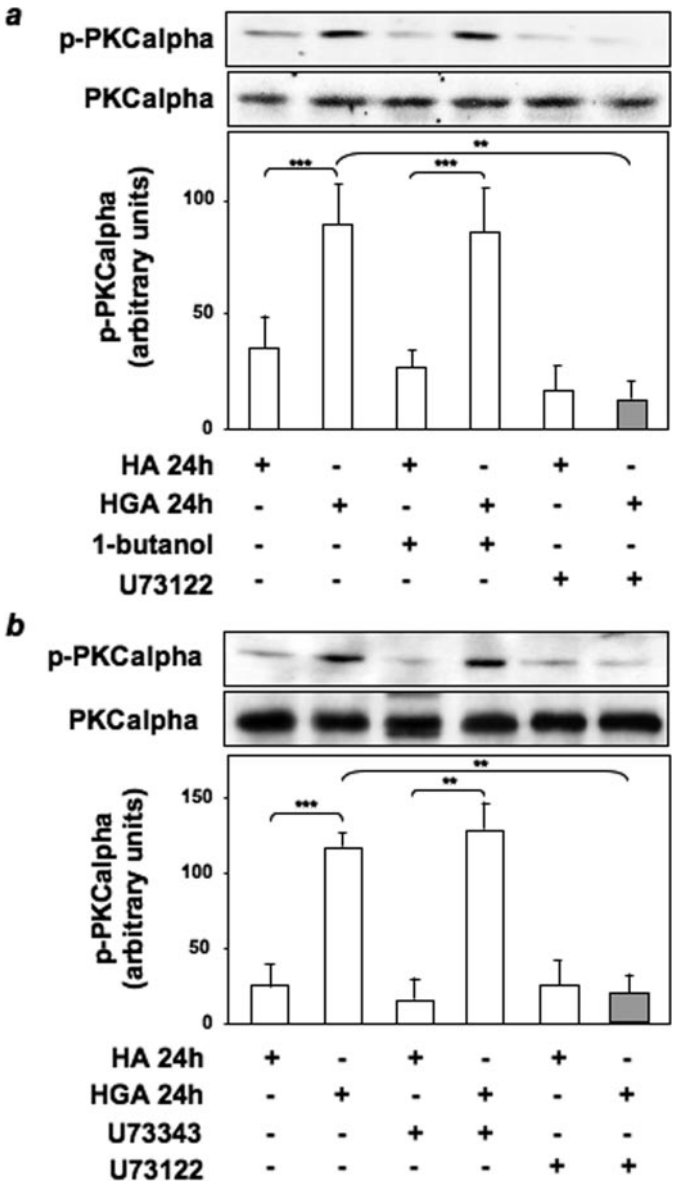

FIGURE 4. **Role of PLC and PLD in HGA-induced PKCα activation in L6 skeletal muscle cells.** Cell lysates of L6 skeletal muscle cells incubated with 0.1 mg/ml HA or HGA for 24 h in the absence or in the presence of 0.3% 1-butanol or 10 μM U73122 (*a*) or 5 μM U73343 (*b*) were then immunoprecipitated with anti-PKCα antibody and immunoblotted with antibodies to phospho-PKCα or to PKCα. The autoradiographs shown are representative of three independent experiments. *, statistically significant differences (**, $p < 0.01$; ***, $p < 0.001$).

Western blotting of RAGE immunoprecipitates with antibodies against PKCβ, PKCζ, and PKCδ revealed that these PKC isoforms did not co-precipitate with RAGE after HGA treatment for 24 h. By contrast, HGA induced the association of RAGE with PKCα (Fig. 5*b*). Furthermore, RAGE-associated PKCα activity increased in a time-dependent manner after HGA incubation, reaching a 2-fold increase after 24 h (Fig. 5*c*). Thus, upon AGEs treatment RAGE may form a multimolecular complex including Src and PKCα. Next, cell lysates were precipitated with RAGE antibodies and tested in overlay assays for their ability to bind recombinant biotinylated PKCα. Two major bands of 180 and 65 kDa were revealed upon HGA stimulation of the cells, whereas no bands corresponding to the

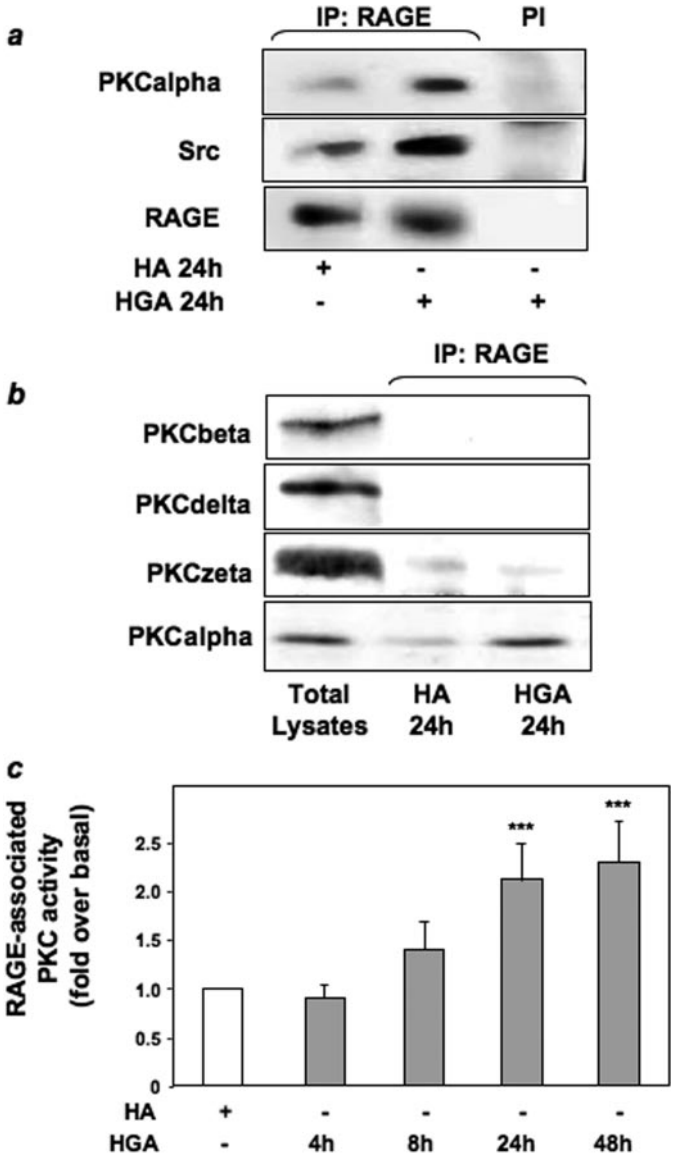

FIGURE 5. **HGA-induced association of PKCα, Src, and RAGE in L6 skeletal muscle cells.** *a*, lysates from L6 skeletal muscle cells treated or not with 0.1 mg/ml HA or HGA for 24 h were precipitated (*IP*) with preimmune serum (*PI*) or with selective anti-RAGE antibodies and immunoblotted with anti-PKCα, anti-Src, or anti-RAGE antibodies. The autoradiographs shown are representative of three independent experiments. *b*, lysates from L6 skeletal muscle cells treated as above were precipitated with selective anti-RAGE antibodies and immunoblotted with PKCβ, PKCδ, PKCζ, or PKCα antibodies. The autoradiographs shown are representative of three independent experiments. *c*, L6 skeletal muscle cells were treated with 0.1 mg/ml HA or HGA for the indicated times. Cells were lysed, cell lysates were then precipitated with selective anti-RAGE antibodies, and PKC activity was measured as described under "Experimental Procedures." *Bars* represent the mean ± S.D. of values obtained from three independent experiments in duplicate. *, statistically significant differences (***, $p < 0.001$).

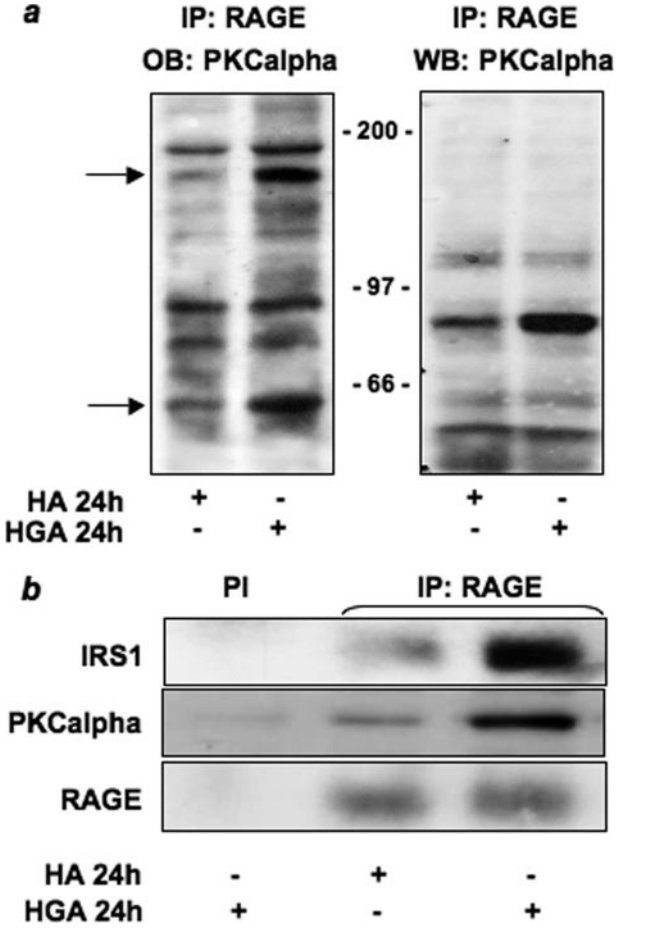

FIGURE 6. **HGA induced the association of IRS-1 with PKCα and RAGE in L6 cells.** *a*, L6 skeletal muscle cells were treated with 0.1 mg/ml HA or HGA for 24 h. Cells were lysed as described under "Experimental Procedures," and lysates were then precipitated (*IP*) with selective anti-RAGE antibodies and loaded on SDS-PAGE. Gels were then transferred onto nitrocellulose filters and incubated with recombinant biotinylated PKCα (*OB PKCα*) as described under "Experimental Procedures" (*left panel*). Cell lysates precipitated with selective anti-RAGE antibodies were also immunoblotted (*WB*) with PKCα antibody (*right panel*). The autoradiographs shown are representative of three independent experiments. *b*, lysates from L6 skeletal muscle cells treated as above were precipitated with pre-immune serum (*PI*) or selective anti-RAGE antibodies and loaded on SDS-PAGE. Gels were then transferred on nitrocellulose filters and immunoblotted with anti-IRS1, anti-PKCα, or anti-RAGE antibodies. The autoradiographs shown are representative of three independent experiments.

molecular mass of RAGE were detected (Fig. 6*a*). This indicates that RAGE/PKCα is not a direct interaction. Both the apparent molecular mass and mass spectrometric analysis indicated that the 180-kDa species corresponded to IRS-1, whereas the 65-kDa was identified as c-Src. Western blot with anti-IRS-1 and anti-PKCα antibodies performed on immunoprecipitates anti-RAGE revealed that HGA treatment increased RAGE co-precipitation with both IRS-1 and PKCα (Fig. 6*b*).

Role of IRS-1 and Src in PKCα and RAGE Association in L6 Skeletal Muscle Cells—To address the functional role of IRS-1 and Src in the activation of PKCα induced by HGA, we evaluated the effect of IRS-1 or Src inhibition on RAGE/PKCα association. L6 cells were transfected with a specific IRS-1-ribozyme (39), which specifically inhibited IRS-1 expression by about 80% without affecting PKCα levels (Fig. 7*a*). In untransfected L6 cells, 24 h of HGA treatment induced the association of RAGE with PKCα (Fig. 7*b*). Interestingly, the transfection of IRS-1-ribozyme abolished HGA-induced RAGE/PKCα co-precipitation (Fig. 7*b*). Furthermore, ribozyme-mediated inhibition of IRS-1 expression blocked the RAGE-associated PKC activity induced by HGA (Fig. 7*c*). The general PKC inhibitor bisindolyl maleimide was used as a control of PKC activity (Fig. 7*c*).

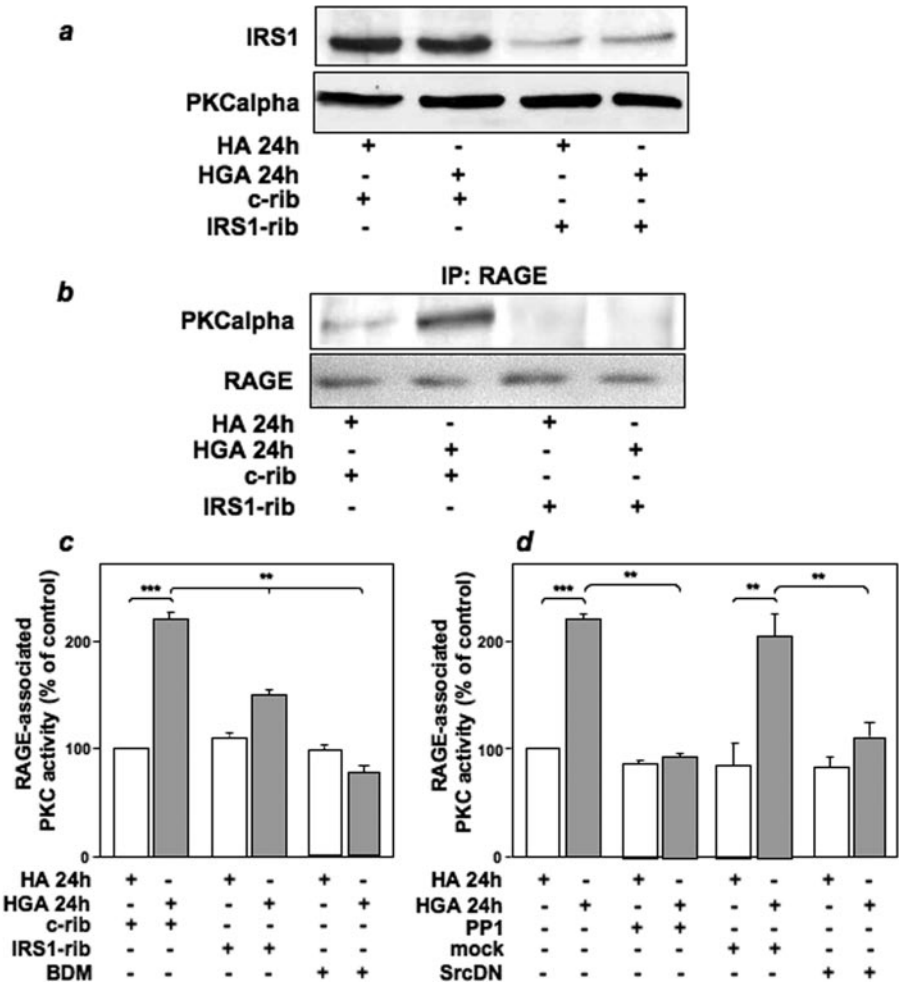

FIGURE 7. **IRS-1 and Src are necessary for HGA-induced association of PKCα and RAGE in L6 cells.** *a*, L6 skeletal muscle cells were transfected with a specific IRS-1-ribozyme (*IRS1-rib*) or a control ribozyme (*c-rib*) as described under "Experimental Procedures." Cells were then treated or not with 0.1 mg/ml HA or HGA for 24 h. Cells were lysed as described under "Experimental Procedures," and lysates were then immunoblotted with IRS1 or PKCα antibodies. The autoradiographs shown are representative of three independent experiments. *b*, lysates from L6 skeletal muscle cells treated as above were precipitated (*IP*) with selective RAGE antibodies and loaded on SDS-PAGE. Gels were then transferred on nitrocellulose filters and immunoblotted with PKCα or RAGE antibodies. The autoradiographs shown are representative of three independent experiments. *c*, L6 skeletal muscle cells were transfected with a specific IRS-1-ribozyme (*IRS-1-rib*) or a control ribozyme (*c-rib*) as described under "Experimental Procedures" then treated or not with 0.1 mg/ml HA or HGA for 24 h in the absence or presence of 100 nM bisindolyl maleimide. Cells were lysed, cell lysates were then precipitated with selective anti-RAGE antibodies, and PKC activity was measured as described under "Experimental Procedures". *d*, L6 skeletal muscle cells were incubated with 0.1 mg/ml HA or HGA for 24 h in the absence or in the presence of 5 μM PP1. Alternatively, L6 skeletal muscle cells were also mock-transfected or transfected with a kinase-inactive dominant negative Src (*SrcDN*), as described under "Experimental Procedures" and then incubated with 0.1 mg/ml HA or HGA for 24 h. Cells were lysed, cell lysates were then precipitated with selective anti-RAGE antibodies, and PKC activity was measured as described under "Experimental Procedures." *Bars* represent the mean ± S.D. of three independent experiments. *, statistically significant differences (**, $p < 0.01$, ***, $p < 0.001$).

These results suggest a key role of IRS-1 in mediating RAGE/PKCα interaction. Moreover, inhibition of Src activity by PP1 or the SrcDN prevented the stimulatory effect of HGA on RAGE-associated PKCα activity (Fig. 7*d*).

Effect of Dietary AGEs on Body Weight, Food Intake, and Fasting Blood Metabolite Levels—C57/BL6 mice were fed either LAD or HAD. As assessed by detection of CML-like immunoepitopes, AGE content was about 3-fold higher in HAD compared with LAD (data not shown). Because the daily food intake was equal between HAD- and LAD-fed mice (Table 3), HAD-fed mice ingested ~3-fold more CML than the LAD-fed mice. This was reflected in part in the fasting serum CML-adducts levels, which were 2-fold higher in HAD-fed animals than in LAD-fed animals (LAD-fed mice 68 ± 8 units/ml *versus* HAD-fed mice 131 ± 6 units/ml; $n = 8$/group, $p < 0.02$). Thus, steady-state serum levels of AGEs were consistent with the estimated content in the dietary formulas. Mice from either diet group showed no significant differences in body weight measured during the entire period of diet (Table 3). Within 11 weeks of treatment, fasting glucose levels in HAD-fed mice were significantly increased by 1.3-fold as compared with LAD-fed mice and became 1.5-fold higher up to 22 weeks of diet. At week 22, HAD-fed mice also featured a 1.4-fold increase in fasting insulin levels compared with LAD-fed animals (Table 3). Similarly, fasting non-esterified free fatty acid and triglyceride blood concentrations in HAD-fed mice were increased by 1.25- and 1.60-fold, respectively, suggesting the presence of insulin resistance in these animals (Table 3). Interestingly, fasting non-esterified free fatty acid and triglycerides in mice were also increased by 1.3-fold after 9 weeks of HAD despite no significant differences in fasting glucose levels (Table 3).

Glucose Tolerance and Insulin Sensitivity in HAD- and LAD-fed Mice—We then investigated the effect of HAD on glucose tolerance by intraperitoneal glucose loading (2 mg/kg) at week 22. In HAD-fed mice, blood glucose levels remained significantly higher than in LAD-fed mice (area under the curve, 7680 ± 3200 in HAD-fed mice *versus* 4791 ± 1770 in LAD-fed mice, $p < 0.05$). To determine possible alterations in insulin sensitivity, we performed insulin tolerance tests. In LAD-fed mice, intraperitoneal injection of insulin (0.75 milliunits/g of body weight) caused a severe decrease in blood glucose levels. This decrease achieved a maximum (70%; $p = 0.005$) after 45 min and was maintained for further 75 min. At variance, insulin reduced glucose levels by only 50% after 45 min in HAD-fed mice followed by a progressive rescue of the initial blood glucose concentration over the following 75 min (area under the curve, 9848 ± 3000 in HAD-fed mice *versus* 5267 ± 1700 in LAD-fed mice, $p < 0.0001$) (Fig. 8*a*). Insulin sensitivity was already

TABLE 3

Mice were analyzed as described under "Experimental Procedures." Data are the the means ± S.D. of determinations in 12 LAD- and 12 HAD-fed mice

	LAD				HAD			
	Base line	Week 9	Week 11	Week 22	Base line	Week 9	Week 11	Week 22
Food intake (g/day)	3.30 ± 0.10	3.46 ± 0.20	3.44 ± 0.14	4.30 ± 0.24	3.50 ± 0.22	3.88 ± 0.15	3.58 ± 0.15	4.04 ± 0.20
Weight (g)	14.3 ± 2.2	20.4 ± 1.0	20.8 ± 1.6	23.1 ± 1.7	14.4 ± 1.8	20.4 ± 0.9	20.5 ± 1.6	22.2 ± 0.8
Fasting blood glucose (mg/dl)	69 ± 13	69 ± 22	79 ± 16	80 ± 12	68 ± 10	78 ± 12	103 ± 15[a]	117 ± 12[b]
Fasting serum insulin (mmol/liter)	ND	ND	ND	4.99 ± 1.18	ND	ND	ND	7.48 ± 2.70[a]
Fasting NEFA (mmol/liter)	ND	0.35 ± 0.07	ND	0.43 ± 0.08	ND	0.45 ± 0.02[c]	ND	0.53 ± 0.09[c]
Fasting triglycerides (mg/ml)	ND	0.49 ± 0.02	ND	0.59 ± 0.12	ND	0.64 ± 0.07[c]	ND	0.95 ± 0.27[c]

[a] $p < 0.01$.
[b] $p < 0.001$.
[c] $p < 0.05$.

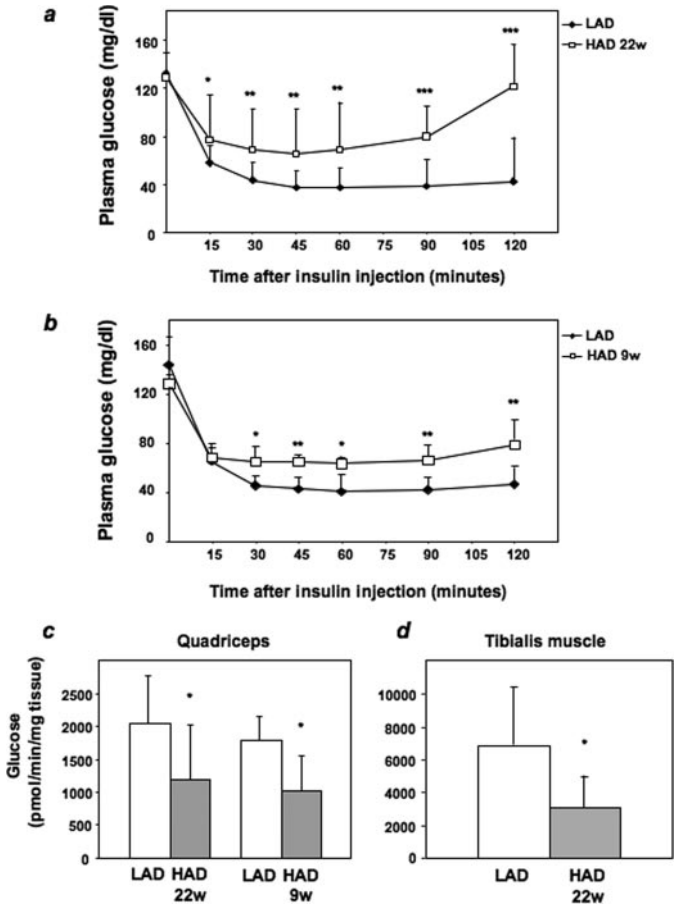

FIGURE 8. **Insulin sensitivity and glucose transport in LAD- and HAD-fed mice.** *a*, 4-week-old female mice of the C57/BL6 strain were fed a LAD or a HAD diet as described under "Experimental Procedures." At week (*w*) 22 (*a*) and week 9 (*b*) mice were injected intraperitoneally with insulin (0.75 milliunits/g of body weight) followed by determinations of blood glucose levels at the indicated times. Values are expressed as the means ± S.D. *c* and *d*, mice fed LAD or HAD for 9 or 22 weeks were subjected to intravenous injection of 1 μCi of 2-deoxy-D-[1-^{3}H]glucose and intraperitoneal injection of insulin. Quadriceps (*c*) or tibialis (*d*) muscles were removed 30 min after and snap-frozen in liquid nitrogen. 2-Deoxy-D-[1-^{3}H]glucose accumulated in muscle tissues was quantitated as described under "Experimental Procedures." *Bars* represent mean values ± S.D. of determinations in at least seven mice/group. *, statistically significant differences (*, $p < 0.05$; **, $p < 0.01$; ***, $p < 0.001$).

reduced in mice after 9 weeks of HAD, as shown in Fig. 8*b* (area under the curve, 8522 ± 2419 in HAD-fed mice *versus* 5920 ± 1215 in LAD-fed mice, $p < 0.01$).

Effect of HAD on Glucose Uptake, PKB/Akt, and PKCα Activation in Vivo—In cultured L6 skeletal muscle cells, incubation with HGA causes resistance to insulin action on glucose uptake (31). We, therefore, tested whether HAD also impairs insulin stimulation of the glucose transport machinery *in vivo*. Insulin-stimulated glucose uptake in the quadriceps and tibialis muscles from 22-week HAD-fed animals was decreased by 42 and 56%, respectively, compared with the LAD-fed mice (Fig. 8, *c* and *d*). Insulin-stimulated glucose uptake was reduced also in the quadriceps from 9-week HAD-fed mice (Fig. 8*c*). In parallel with the decreased glucose uptake, phosphorylation of PKB/Akt in response to insulin was also significantly reduced in skeletal muscles from HAD-fed mice (Fig. 9, *a* and *b*). This abnormality was accompanied by no significant change in the total PKB/Akt levels. We have previously demonstrated that the negative effects of HGA on insulin metabolic signaling in L6 myotubes are specifically mediated by PKCα (31). We, therefore, measured PKCα-specific activity in muscles from both HAD- and LAD-fed mice. As shown in Fig. 9*c*, PKCα specific activity measured in fasting conditions was increased by 2.3- and 1.8-fold in muscles from 22- and 9-week HAD-fed mice, respectively, compared with LAD-fed mice. Thus, AGEs modulate insulin signaling and PKCα activity *in vivo* as well as in cultured cells.

HAD-induced Src Activation and Association of PKCα, Src, and RAGE in Mice Skeletal Muscles—To investigate the ability of HAD to activate Src and to induce the formation of the complex between Src, RAGE, and/or PKCα *in vivo*, muscle tissue lysates from HAD- or LAD-fed mice were blotted with anti-phospho-Src Tyr^{416} antibody. An ~2-fold increase of Src phosphorylation was observed in tibialis muscle from both 9- and 22-week HAD-fed mice compared with LAD-fed mice (Fig. 10). Furthermore, as shown in Fig. 11, RAGE coprecipitation with both Src and PKCα was increased in lysates from muscles from C57/BL6 HAD-fed mice when compared with LAD-fed mice. An increase of RAGE-associated PKCα activity was also observed in HAD fed mice (data not shown).

Glycated Albumin-induced PKCα and Src Activation in Mice Skeletal Muscles—To further support the role of AGEs in the activation of both PKCα and Src *in vivo*, C57/BL6 mice were injected with HGA either directly in the skeletal muscle (GA-Im) or in the tail vein (GA-Iv) as described under "Experimental Procedures." Muscle tissue lysates from GA-Im and GA-Iv mice were blotted with either anti-phospho PKCα (Fig. 12, *a*, *c*, *e*, and *g*) or Src Tyr^{416} antibody (Fig. 12, *b*, *d*, *f*, and *h*). An ~2-fold increase of both PKCα (Fig. 12, *a* and *c*) and Src phosphorylation (Fig. 12, *b* and *d*) was observed in quadriceps from GA-Im mice compared with mice treated with vehicle alone

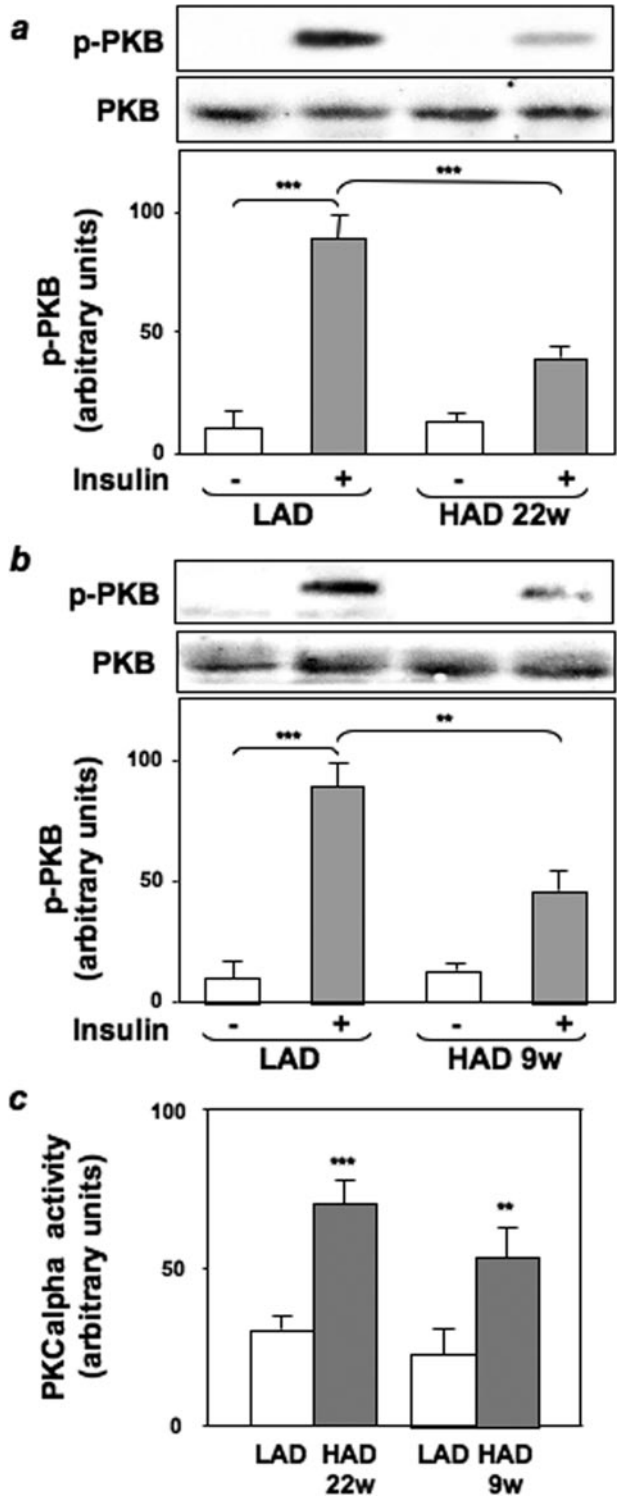

FIGURE 9. **Effect of LAD and HAD on PKB/Akt and PKCα activation *in vivo*.** *a*, 4-week-old female mice of the C57/BL6 strain were fed a LAD or a HAD diet as described under "Experimental Procedures." At week (*w*) 22 (*a*) and week 9 (*b*), mice were injected intraperitoneally with insulin (0.125 milliunits/g of body weight), and muscle tissues were collected and homogenized. Tissue homogenates were subjected to SDS-PAGE followed by immunoblotting with antibodies to phosphoserine 473 PKB/Akt and to PKB/Akt as a control. PKB/Akt phosphorylation was analyzed by densitometry. *Bars* represent the mean ± S.D. of three different experiments. *c*, at week 9 or at week 22 muscle tissues homogenates were subjected to immunoprecipitation with PKCα antibodies, and specific PKCα activity was measured as described under "Experimental Procedures." *Bars* represent the mean ± S.D. of three independent experiments. *, statistically significant differences (**, $p < 0.01$; ***, $p < 0.001$).

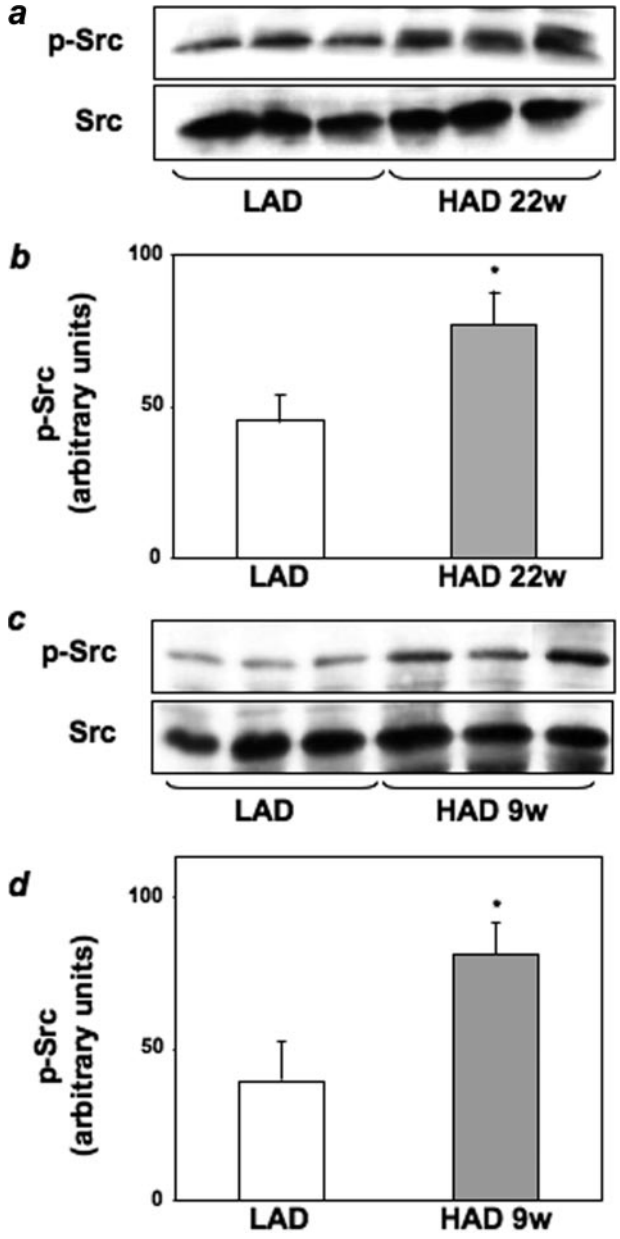

FIGURE 10. **Effect of LAD and HAD on Src activation *in vivo*.** *a*, tibialis muscle homogenates from 22 weeks (*w*) LAD- or HAD-fed mice were separated by SDS-PAGE followed by immunoblotting with antibodies to phosphotyrosine 416 Src or total Src. The autoradiographs shown are representative of three independent experiments. *b*, densitometric analysis of phosphotyrosine 416 Src normalized on total Src. *c*, tibialis muscle homogenates from 9-week LAD- or HAD-fed mice were separated by SDS-PAGE followed by immunoblotting with antibodies to phosphotyrosine 416 Src or total Src. The autoradiographs shown are representative of three independent experiments. *d*, densitometric analysis of phosphotyrosine 416 Src normalized on total Src. *, statistically significant differences (*, $p < 0.05$).

(PBS) or with non-glycated albumin (HA). Furthermore, both PKCα (Fig. 12, *e* and *g*) and Src phosphorylation (Fig. 12, *f* and *h*) were increased by 2.5- and 1.8-fold, respectively, in muscle lysates from GA-Iv mice when compared with PBS or HA-treated mice.

DISCUSSION

We have previously shown that in L6 skeletal muscle cells chronic exposure to HGA selectively inhibits the phosphatidyl-

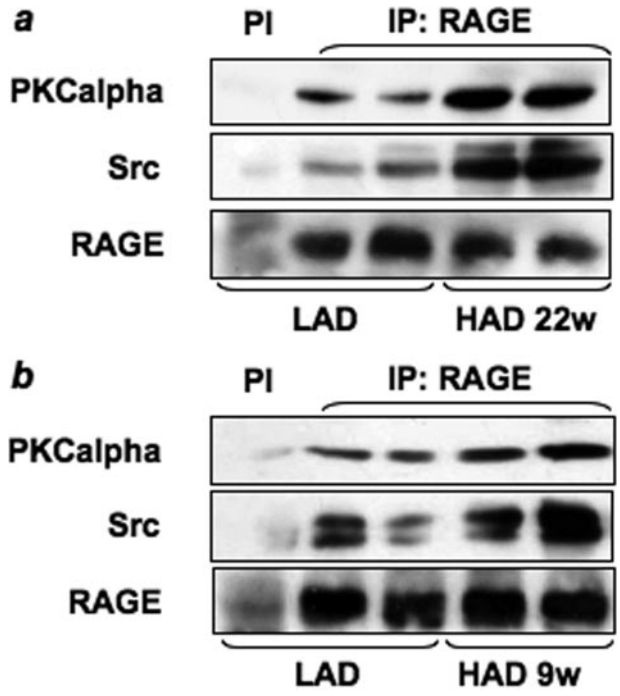

FIGURE 11. **Effect of LAD and HAD on PKCα, Src, and RAGE association *in vivo*.** Tibialis muscle homogenates from mice fed LAD or HAD for 22 weeks (*w*) (*a*) or for 9 weeks (*b*) were precipitated (*IP*) with preimmune serum (*PI*) or with selective anti-RAGE antibodies and immunoblotted with anti-PKCα, anti-Src or anti-RAGE antibodies. The autoradiographs shown are representative of four independent experiments.

inositol 3-kinase/PKB pathway in the insulin signaling cascade while leaving the Ras-ERK activation and mitogenic action of the hormone unaltered (31). In L6 myotubes the HGA-induced alteration of insulin metabolic signals is paralleled by an increase of serine/threonine phosphorylation of the IRSs specifically mediated by the activation of PKCα independently of reactive oxygen species (31). Previous studies have shown that the PKC family of serine/threonine kinases is implicated in development of insulin resistance (40, 41). The PKC family is composed of several isoforms, divided into three groups according to their structure and activation mechanisms (42). The atypical isoforms play a positive role in glucose transport (43), whereas classical isoforms are involved in generation of insulin resistance. It is well established that PKCα and -β are able to phosphorylate insulin receptor and IRSs on serine and threonine residues, inhibiting their tyrosine phosphorylation (44–46).

Importantly, our studies revealed that in L6 cells inhibition of Src kinase, either by a specific pharmacological inhibitor such as PP1 or by transfecting a dominant negative form of the kinase, prevents the HGA-induced increase in PKCα activity, suggesting a key role for Src in this event. Interestingly, PKCα is tyrosine-phosphorylated upon HGA treatment, and its tyrosine phosphorylation is abolished by preincubation of L6 cells with PP1. Thus, Src may directly regulate PKCα activity in response to HGA. Furthermore, these effects appear to be RAGE-mediated as a soluble form of RAGE was able to prevent both HGA-induced Src and PKCα activation. PKC activity is implicated in v-Src-induced intracellular signals. In the rat large intestine 1,25-dihydroxyvitamin stimulates the physical association of activated c-Src with PLCγ and activates two Ca^{2+}-dependent PKC isoforms (47). Similarly, activation of v-Src in BALB/c 3T3 cells rapidly increases the intracellular second messenger, DAG via a type D phospholipase/PA phosphatase-mediated signaling pathway (48). These results are consistent with our findings that HGA caused a Src-dependent increase in the amount of DAG in L6 skeletal muscle cells. Moreover, we show that treatment of L6 cells with the pharmacological inhibitor of PLC, U73122, but not its inactive structural analogue U73343, almost completely abolishes HGA-induced PKCα phosphorylation, indicating that, in response to HGA, Src may increase the amount of DAG via PLC. Thus, Src may control PKCα activity by direct phosphorylation and by regulation of DAG intracellular levels via PLC.

HGA-induced increase in DAG levels is not sufficient to activate other PKC isoforms, as we have already described (31). Previous work by Zang *et al.* (49) demonstrated that in cells expressing the oncogenic v-Src, increased production of DAG is accompanied by a selective activation of the α and δ isoforms of PKC, whereas the ϵ isoform is not activated. Furthermore, Pula *et al.* (50) have shown that in platelets PKCα but not PKCβ was activated in an Syk- and phospholipase C-dependent manner. It has been proposed that specific DAG species are generated to activate specific PKC isoforms. Indeed, several reports have demonstrated that different stimuli generate different DAG species, and PKC isotypes are differentially sensitive to the fatty acid composition of DAG (51). Thus, it is possible that in L6 cells the lack of activation of other PKC isoforms is due to specific DAG produced by HGA stimulation.

We then hypothesized that HGA could activate Src via RAGE. Reddy *et al.* (30) showed that S100B activates Src kinase in a RAGE-dependent manner and that Src kinase is required for the S100B-induced RAGE signaling, leading to migration and inflammatory gene expression in vascular smooth muscle cells. Co-localization of RAGE and Src has been evidenced in caveolae (30), where Cav-1 plays an important role in the assembly and integration of signaling complexes (52, 53). It is well known that RAGE can activate several downstream signaling pathways, including ERK1/2, phosphatidylinositol 3-kinase, PKC, the Janus tyrosine kinases (JAKs), and transcription factors, including STAT3, AP1, and NF-κB (22, 26). Moreover, the cytoplasmic region of RAGE is responsible for the binding of the signaling molecule(s). In intact cells, ERK1/2 have been identified as RAGE-binding proteins. Binding to the intracellular region of RAGE localizes ERK under the proximal region of the plasma membrane, enabling the interaction between ERK and its substrates (27). Our results are consistent with the hypothesis that the formation of a multimolecular complex, involving RAGE, PKCα, and Src kinase, occurs in response to chronic HGA treatment. Indeed, coprecipitation experiments showed that in L6 cells Src kinase interacts with both RAGE and PKCα. RAGE cytoplasmic domain might also be involved in the interaction of RAGE with both Src and PKCα. Fine mapping of the interaction sites between Src, PKCα, and RAGE is currently under investigation in our laboratory.

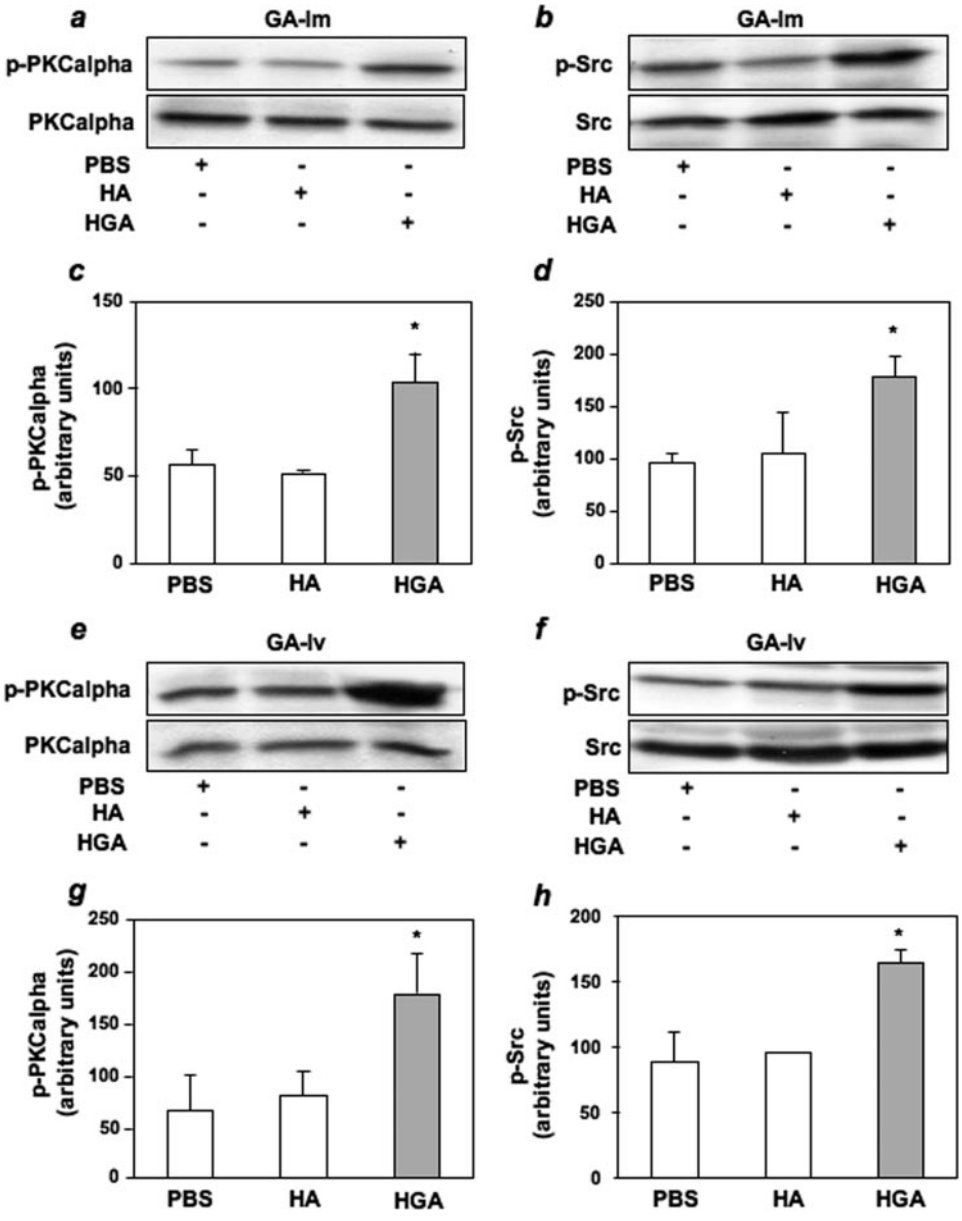

FIGURE 12. **Effect of glycated albumin on PKCα and Src activation *in vivo*.** 4-Week-old female mice of the C57/BL6 strain were injected with 50 mg/kg of HGA or HA or PBS either directly in the quadriceps (*GA-Im*: *a*, *b*, *c*, and *d*) or in the tail vein (*GA-Iv*: *e*, *f*, *g*, and *h*) as described under "Experimental Procedures. *a* and *c*, muscle tissue lysates from muscle-injected mice were blotted with anti-phospho PKCα, and PKCα phosphorylation was analyzed by densitometry. *b* and *d*, muscle tissue lysates from muscle-injected mice were blotted with anti-phospho Src Tyr^{416} antibody and Src phosphorylation was analyzed by densitometry. *e* and *g*, muscle tissue lysates from tail vein-injected mice were blotted with anti-phospho PKCα, and PKCα phosphorylation was analyzed by densitometry. *f* and *h*, muscle tissue lysates from tail vein-injected mice were blotted with anti-phospho-Src Tyr^{416} antibody, and Src phosphorylation was analyzed by densitometry. A representative autoradiograph is shown. *Bars* represent the mean ± S.D. of three different experiments. *, statistically significant differences (*, $p < 0.05$).

Overlay blot assays revealed that, in response to HGA, a 180-kDa protein, identified as IRS-1, and Src may directly bind PKCα. Thus, HGA may induce direct interaction of PKCα with IRS1 and Src. IRS1, or less likely Src, in turn may bridge RAGE interaction with PKCα, the latter two having no direct interaction. Indeed, our experiments in L6 cells transfected with IRS-1 ribozyme indicate that IRS-1 is required for RAGE-PKCα co-precipitation and activation in response to HGA. This is consistent with our previous findings showing that IRS-1 but not IRS-2 expression is necessary to allow classical PKC activation in response to insulin (39). Thus, one might speculate that, in response to different stimuli, PKCα is involved in the formation of different specific multimolecular complexes, which modulate insulin sensitivity. In this paper we also provide evidence that dietary AGEs are able to affect insulin sensitivity and glucose tolerance *in vivo*. These effects were AGEs-specific and not caused by hyperglycemia, as C57/BL6 mice fed a HAD for 9 weeks show a reduction of insulin sensitivity despite no significant differences in fasting glucose levels (Table 3). Prolonged exposure to HAD subsequently led to higher fasting glucose levels after 11 weeks of diet up to the end of the treatment compared with mice fed a LAD despite equal food intake and weight gain. Throughout this period HAD-fed mice appear consistently hyperinsulinemic in fasting conditions and exhibit increased non-esterified free fatty acid and triglycerides levels compared with LAD-fed mice. Because glucose tolerance is also slightly impaired at 22 weeks of HAD, it is conceivable that dietary AGEs affect insulin secretion in addition to insulin action. This is consistent with the evidence that accumulation of islet AGEs could be important for glucotoxicity toward β-cells (54). Furthermore, insulin-induced PKB phosphorylation and glucose uptake are dramatically reduced in tibialis and quadriceps muscles of HAD-fed mice. Impairment of insulin metabolic signaling is accompanied by an increase in PKCα specific activity in tibialis muscles from the HAD-fed mice, showing again that the mechanism by which HGA exacerbates the insulin-resistant state in intact cells also occurs *in vivo*. Moreover, an increase in PKCα specific activity in tibialis muscles from the HAD-fed mice appeared to be associated to the increase of the RAGE-PKCα-Src complex formation. Increases of both PKCα and Src phosphorylation were also observed when HGA was delivered either by direct intramuscular or by intravenous injection in mice. These observations further support the *in vivo* relevance of HGA and the conclusion that the differences in LAD- and HAD-fed mice are largely due to AGEs. In summary, our data suggest that AGEs-induced PKCα activity in the muscle might be mediated by the forma-

tion of a RAGE-PKCα-Src-IRS1 complex both *in vitro* and *in vivo*.

Acknowledgments—We thank Dr. Angelika Bierhaus for kindly providing the sRAGE and Prof. Eduardo Consiglio for helpful discussion and critical reading of the manuscript. We also thank Dr. Gregory A. Raciti for critical reading of the manuscript.

REFERENCES

1. Kahn, B. B., and Flier, J. S. (2000) *J. Clin. Investig.* **106,** 473–481
2. Hager, S. R., Jochen, A. L., and Kalkhoff, R. K. (1991) *Am. J. Physiol.* **260,** E353–E362
3. Davidson, M. B., Bouch, C., Venkatesan, N., and Karjala, R. G. (1994) *Am. J. Physiol.* **267,** E808–E813
4. Idris, I., Gray, S., and Donnelly, R. (2002) *Ann. N. Y. Acad. Sci.* **967,** 176–182
5. Yerneni, K. K., Bai, W., Khan, B. V., Medford, R. M., and Natarajan, R. (1999) *Diabetes* **48,** 855–864
6. Nishikawa, T., Edelstein, D., Du, X. L., Yamagishi, S., Matsumura, T., Kaneda, Y., Yorek, M. A., Beebe, D., Oates, P. J., Hammes, H. P., Giardino, I., and Brownlee, M. (2000) *Nature* **404,** 787–790
7. Hattori, Y., Suzuki, M., Hattori, S., and Kasai, K. (2002) *Hypertension* **39,** 22–28
8. Ruggiero-Lopez, D., Rellier, N., Lecomte, M., Lagarde, M., and Wiernsperger, N. (1997) *Diabetes Res. Clin. Pract.* **34,** 135–142
9. Treins, C., Giorgetti-Peraldi, S., Murdaca, J., and Van Obberghen, E. (2001) *J. Biol. Chem.* **276,** 43836–43841
10. Yamagishi, S., Inagaki, Y., Okamoto, T., Amano, S., Koga, K., Takeuchi, M., and Makita, Z. (2002) *J. Biol. Chem.* **277,** 20309–20315
11. Hoffmann, S., Friedrichs, U., Eichler, W., Rosenthal, A., and Wiedemann, P. (2002) *Graefes Arch. Clin. Exp. Ophthalmol.* **240,** 996–1002
12. Makita, Z., Yanagisawa, K., Kuwajima, S., Yoshioka, N., Atsumi, T., Hasunuma, Y., and Koike, T. (1995) *J. Diabetes Complications* **9,** 265–268
13. Flyvbjerg, A. (2000) *Diabetologia* **43,** 1205–1223
14. O'Brien, J., and Morrissey, P. A. (1989) *Crit. Rev. Food Sci. Nutr.* **28,** 211–248
15. Vlassara, H. (2000) *Hosp. Pract.* **35,** 25–27, 32, 35–39
16. Koschinsky, T., He, C. J., Mitsuhashi, T., Bucala, R., Liu, C., Buenting, C., Heitmann, K., and Vlassara, H. (1997) *Proc. Natl. Acad. Sci. U. S. A.* **94,** 6474–6479
17. He, C., Sabol, J., Mitsuhashi, T., and Vlassara, H. (1999) *Diabetes* **48,** 1308–1315
18. He, C., Li, J., Sabol, J., Hattori, M., Chang, M., Mitsuhashi, T., and Vlassara, H. (2001) *Diabetes* **50 (suppl. 1),** 48
19. Lin, R., Choudhury, R., Lu, M., Dore, A., Fallon, J., Fisher, E., and Vlassara, H. (2001) *Diabetes* **50 (suppl. 2),** 48
20. Hofmann, S. M., Dong, H. J., Li, Z., Cai, W., Altomonte, J., Thung, S. N., Zeng, F., Fisher, E. A., and Vlassara, H. (2002) *Diabetes* **51,** 2082–2089
21. Thornalley, P. J. (1998) *Cell. Mol. Biol.* (*Noisy-le-Grand*) **44,** 1013–1023
22. Bucciarelli, L. G., Wendt, T., Rong, L., Lalla, E., Hofmann, M. A., Goova, M. T., Taguchi, A., Yan, S. F., Yan, S. D., Stern, D. M., and Schmidt, A. M. (2002) *Cell. Mol. Life Sci.* **59,** 1117–1128
23. Schmidt, A. M., Hori, O., Brett, J., Yan, S. D., Wautier, J. L., and Stern, D. (1994) *Arterioscler. Thromb.* **14,** 1521–1528
24. Hofmann, M. A., Drury, S., Fu, C., Qu, W., Taguchi, A., Lu, Y., Avila, C., Kambham, N., Bierhaus, A., Nawroth, P., Neurath, M. F., Slattery, T., Beach, D., McClary, J., Nagashima, M., Morser, J., Stern, D., and Schmidt, A. M. (1999) *Cell* **97,** 889–901
25. Taguchi, A., Blood, D. C., del Toro, G., Canet, A., Lee, D. C., Qu, W., Tanji, N., Lu, Y., Lalla, E., Fu, C., Hofmann, M. A., Kislinger, T., Ingram, M., Lu, A., Tanaka, H., Hori, O., Ogawa, S., Stern, D. M., and Schmidt, A. M. (2000) *Nature* **405,** 354–360
26. Huttunen, H. J., Fages, C., and Rauvala, H. (1999) *J. Biol. Chem.* **274,** 19919–19924
27. Ishihara, K., Tsutsumi, K., Kawane, S., Nakajima, M., and Kasaoka, T. (2003) *FEBS Lett.* **550,** 107–113
28. Brizzi, M. F., Dentelli, P., Gambino, R., Cabodi, S., Cassader, M., Castelli, A., Defilippi, P., Pegoraro, L., and Pagano, G. (2002) *Diabetes* **51,** 3311–3317
29. Cho, H. M., Choi, S. H., Hwang, K. C., Oh, S. Y., Kim, H. G., Yoon, D. H., Choi, M. A., Lim, S., Song, H., Jang, Y., and Kim, T. W. (2005) *Mol. Cell* **19,** 60–66
30. Reddy, M. A., Li, S. L., Sahar, S., Kim, Y. S., Xu, Z. G., Lanting, L., and Natarajan, R. (2006) *J. Biol. Chem.* **281,** 13685–13693
31. Miele, C., Riboulet, A., Maitan, M. A., Oriente, F., Romano, C., Formisano, P., Giudicelli, J., Beguinot, F., and Van Obberghen, E. (2003) *J. Biol. Chem.* **278,** 47376–47387
32. Morcos, M., Sayed, A. A., Bierhaus, A., Yard, B., Waldherr, R., Merz, W., Kloeting, I., Schleicher, E., Mentz, S., Abd el Baki, R. F., Tritschler, H., Kasper, M., Schwenger, V., Hamann, A., Dugi, K. A., Schmidt, A. M., Stern, D., Ziegler, R., Haering, H. U., Andrassy, M., van der Woude, F., and Nawroth, P. P. (2002) *Diabetes* **51,** 3532–3544
33. Miele, C., Raciti, G. A., Cassese, A., Romano, C., Giacco, F., Oriente, F., Paturzo, F., Andreozzi, F., Zabatta, A., Troncone, G., Bosch, F., Pujol, A., Chneiweiss, H., Formisano, P., and Beguinot, F. (2007) *Diabetes* **56,** 622–633
34. Fiory, F., Oriente, F., Miele, C., Romano, C., Trencia, A., Alberobello, A. T., Esposito, I., Valentino, R., Beguinot, F., and Formisano, P. (2004) *J. Biol. Chem.* **279,** 11137–11145
35. Oriente, F., Andreozzi, F., Romano, C., Perruolo, G., Perfetti, A., Fiory, F., Miele, C., Beguinot, F., and Formisano, P. (2005) *J. Biol. Chem.* **280,** 40642–40649
36. Preiss, J. E., Loomis, C. R., Bell, R. M., and Niedel, J. E. (1987) *Methods Enzymol.* **141,** 294–300
37. Miele, C., Paturzo, F., Teperino, R., Sakane, F., Fiory, F., Oriente, F., Ungano, P., Valentino, R., Beguinot, F., and Formisano, P. (2007) *J. Biol. Chem.* **282,** 31835–31843
38. Ulianich, L., Garbi, C., Treglia, A. S., Punzi, D., Miele, C., Raciti, G. A., Beguinot, F., Consiglio, E., and Di Jeso, B. (2008) *J. Cell Sci.* **121,** 477–486
39. Formisano, P., Oriente, F., Fiory, F., Caruso, M., Miele, C., Maitan, M. A., Andreozzi, F., Vigliotta, G., Condorelli, G., and Beguinot, F. (2000) *Mol. Cell. Biol.* **20,** 6323–6333
40. Nakajima, K., Yamauchi, K., Shigematsu, S., Ikeo, S., Komatsu, M., Aizawa, T., and Hashizume, K. (2000) *J. Biol. Chem.* **275,** 20880–20886
41. Ravichandran, L. V., Esposito, D. L., Chen, J., and Quon, M. J. (2001) *J. Biol. Chem.* **276,** 3543–3549
42. Formisano, P., and Beguinot, F. (2001) *J. Endocrinol. Investig.* **24,** 460–467
43. Liu, X. J., He, A. B., Chang, Y. S., and Fang, F. D. (2006) *Cell. Signal.* **18,** 2071–2076
44. Chin, J. E., Dickens, M., Tavare, J. M., and Roth, R. A. (1993) *J. Biol. Chem.* **268,** 6338–6347
45. Kellerer, M., Mushack, J., Seffer, E., Mischak, H., Ullrich, A., and Häring, H. U. (1998) *Diabetologia* **41,** 833–838
46. Bossenmaier, B., Mosthaf, L., Mischak, H., Ullrich, A., and Häring, H. U. (1997) *Diabetologia* **40,** 863–866
47. Khare, S., Bolt, M. J., Wali, R. K., Skarosi, S. F., Roy, H. K., Niedziela, S., Scaglione-Sewell, B., Aquino, B., Abraham, C., Sitrin, M. D., Brasitus, T. A., and Bissonnette, M. (1997) *J. Clin. Investig.* **99,** 1831–1841
48. Song, J. G., Pfeffer, L. M., and Foster, D. A. (1991) *Mol. Cell. Biol.* **11,** 4903–4908
49. Zang, Q., Frankel, P., and Foster, D. A. (1995) *Cell Growth Differ.* **6,** 1367–1373
50. Pula, G., Crosby, D., Baker, J., and Poole, A. W. (2005) *J. Biol. Chem.* **280,** 7194–7205
51. Shirai, Y., and Saito, N. (2002) *J. Biochem.* (*Tokyo*) **132,** 663–668
52. Lisanti, M. P., Scherer, P. E., Vidugiriene, J., Tang, Z., Hermanowski-Vosatka, A., Tu, Y. H., Cook, R. F., and Sargiacomo, M. (1994) *J. Cell Biol.* **126,** 111–126
53. Okamoto, T., Schlegel, A., Scherer, P. E., and Lisanti, M. P. (1998) *J. Biol. Chem.* **273,** 5419–5422
54. Tajiri, Y., Möller, C., and Grill, V. (1997) *Endocrinology* **138,** 273–280